POLITECNICO
MILANO 1863

SCUOLA DI INGEGNERIA INDUSTRIALE
E DELL'INFORMAZIONE

Title

MSc in Space Engineering

Authors:

10723712	**Marcello Pareschi**	**(BSc Aerospace Engineering - Politecnico di Milano)**
10836125	**Daniele Paternoster**	**(BSc Aerospace Engineering - Politecnico di Milano)**
10711624	**Alex Cristian Turcu**	**(BSc Aerospace Engineering - Politecnico di Milano)**
10884250	**Tamim Harun Or**	**(BSc Aerospace Engineering - International Islamic University Malaysia)**

Professor: Camilla Colombo

Academic year: 2023-2024

Abstract

Lorem ipsum dolor sit amet, consectetuer adipiscing elit. Ut purus elit, vestibulum ut, placerat ac, adipiscing vitae, felis. Curabitur dictum gravida mauris. Nam arcu libero, nonummy eget, consectetuer id, vulputate a, magna. Donec vehicula augue eu neque. Pellentesque habitant morbi tristique senectus et netus et malesuada fames ac turpis egestas. Mauris ut leo. Cras viverra metus rhoncus sem. Nulla et lectus vestibulum urna fringilla ultrices. Phasellus eu tellus sit amet tortor gravida placerat. Integer sapien est, iaculis in, pretium quis, viverra ac, nunc. Praesent eget sem vel leo ultrices bibendum. Aenean faucibus. Morbi dolor nulla, malesuada eu, pulvinar at, mollis ac, nulla. Curabitur auctor semper nulla. Donec varius orci eget risus. Duis nibh mi, congue eu, accumsan eleifend, sagittis quis, diam. Duis eget orci sit amet orci dignissim rutrum.

Contents

1. Interplanetary mission

1.1. Symbols

Analisi della missione

A_e	$[m^2]$	area di efflusso totale
ϕ	$[rad]$	angolo di traiettoria del razzo

Analisi della missione 2

A_e	$[m^2]$	area di efflusso totale
ϕ	$[rad]$	angolo di traiettoria del razzo

1.2. Introduction

1.2.1. Description of the problem

The first part of the assignment aims at designing an interplanetary transfer from Mars to asteroid 1036 Ganymed exploiting a powered gravity assist on Earth. The problem is analyzed through the patched conics method, without considering the injection and arrival hyperbolae. The initial and final velocity vector of the satellite are assumed to be the same of the respective celestial body. The two heliocentric legs are calculated through the Lambert problem. The trajectory is selected with the only criteria of minimizing the cost of the mission, assessed through the total ΔV. The latter is computed by summing different contributions:

$$\Delta V_{tot} = \Delta V_1 + \Delta V_2 + \Delta V_3 \tag{1.1}$$

where $\boldsymbol{V}_{-,i}$ and $\boldsymbol{V}_{+,i}$ are the velocity vectors before and after the i-th manoeuvre respectively.
Where the three terms are defined as:

- ΔV_1 related to the injection in the first heliocentric leg;
- ΔV_2 related to the exit from the second heliocentric leg;
- ΔV_3 related to the impulse given by the engine at pericentre of hyperbola fly-by;

All the manoeuvres are assumed to be impulsive, i.e. they change only the velocity vector of the spacecraft, mantaining invariated the position vector. Note that ΔV_1 and ΔV_2 are related to heliocentric velocities, while ΔV_3 is calculated through relative geocentric velocities.
For each manoeuvre the cost is computed as:

$$\Delta V_i = \|\boldsymbol{V}_{+,i} - \boldsymbol{V}_{-,i}\| \tag{1.2}$$

1.2.2. Assigned data and constraints

A few constraints were considered:

- earliest departure date $t_{min,dep}$ = [01/01/2028 00 : 00 : 00] in Gregorian calendar
- latest arrival date $t_{max,arr}$ = [01/01/2058 00 : 00 : 00] in Gregorian calendar
- time of flights of the two heliocentric arcs must be greater than the associated parabolic time
- minimum pericentre radius of the fly-by hyperbola $r_p = r_E + 500\ km$
- single-revolution Lambert problem was considered
- reasonable total time of the mission

Note that the constraint on the pericentre radius of the fly-by is considered both for avoid impact on Earth and to prevent undesired atmospheric drag effects.

1.3. Algorithms description

The targeting problem previously defined can be seen as an optimization problem with three degrees of freedom (DOFs). Indeed, once the departing date and the two times of flight of the heliocentric legs are chosen, both the Lambert's arcs and the fly-by hyperbola are fully defined. Regarding the formulation of the Lambert's problem, it requires the knowledge of the initial and final position and also the imposed time of flight between them. For two Lambert's arcs it would be needed a total of six DOFs, but this quantities are dependant one to each other:

- the final position vector of the first arc corresponds to the initial position of the second one;
- the initial date for the departing on the second arc corresponds the arrival date on the first arc;
- fixing the first Lambert's arc, the final position and arrival date for the second Lambert's arc are related through the analytical ephemerides.

Once the two heliocentric legs are determined, the powered gravity assist follows as the geocentric velocity vectors are known.
The method implemented to solve the optimization problem is the **brute force algorithm** refined with the **gradient descent algorithm**. Then, to validate the results, the **brute force algorithm** has been used solely with a more dense search grid in a reasonable domain.

1.3.1. Refined brute force algorithm

Algorithm 1 Bruteforce algorithm

Require: $T_{dep}, \Delta T_1, \Delta T_2$
  $\Delta V_{min} = 10^{10}$
  for i in T_{dep} **do**
    for j in ΔT_1 **do**
      Calculate T_{fly-by}
      Calculate first Lambert's arc
      Calculate Mars' velocity at T_{dep}
      Calculate ΔV_1
      for k in ΔT_2 **do**
        Calculate T_{arr}
        Calculate second Lambert's arc
        Calculate Asteroid's velocity at T_{arr}
        Calculate ΔV_2, ΔV_3, ΔV_{tot}
        if $\Delta v_{tot} < \Delta v_{min}$ and $r_p > r_{Earth} + 500\ km$ **then**
          $\Delta v_{min} = \Delta v_{tot}$
          $T_{dep,min} = T_{dep}$
          $T_{fb,min} = T_{fb}$
          $T_{arr,min} = T_{arr}$
        end if
      end for
    end for
  end for

  Minimize cost using *fminunc* with initial guess $\left(T_{dep,min}; T_{fb,min}; T_{arr,min}\right)$
  return ΔV_{min}; $T_{dep,min}$; $T_{fb,min}$; $T_{arr,min}$

The presented Algorithm 1 is reliable, yet computationally demanding since the research of the minimum is performed through a triple-nested *for* loop. The time of the execution highly depends on the refinement chosen for the three selected periods of time. From this considerations and also noticing that the function to minimize presents high irregularities, it is clear that narrow time windows can help in the overall research. Moreover, with this last observation, it is possible to use a less fine grid of research, since it is reasonable to think that the function will present less irregularities.
As a consequence, it was decided to perform a physical analysis (section 1.4) in order to wisely reduce the time domains for departure, fly-by and arrival. The idea of Algorithm 1 is that, once this reduction is performed, the brute-force search can be carried out on a small but refined grid. To speed up the process and refine the solution, *fminunc* of *MATLAB* was used. The selected initial guess is the outcome of the brute force research.
In order to completely validate the results, the robustness of the brute force algorithm has been exploited. Referring to Algorithm 1, *fminunc* was removed after the for-loop search and the research grid was refined. Moreover, with this computation it is possible to validate the time reduction analyzed in section 1.4.

1.4. Reduction of the time windows

1.4.1. Resonance period analysis

The first natural reduction on the domain of interest that could come to mind is to search the frequency on which the three celestial bodies repeat the relative positions on their orbits. On the approximation of circular orbits, this particular time period would be the synodic period generalized for the case of three bodies. However, this path is unviable because the orbit of the asteroid has a relevant eccentricity. To better comprehend the problem of having that eccentricity, particular attention have to be paid on the definitions of phasing and synodic period for two bodies:

- **Phasing** $\phi \rightarrow$ the angle between two celestial bodies, calculated as the difference in their **true anomalies**:

$$\phi(t) = \theta^{(2)}(t) - \theta^{(1)}(t) \tag{1.3}$$

- **Synodic period** $T_{syn} \rightarrow$ if two celestial bodies have initial phasing ϕ_0, they will return to the same phasing after a synodic period T_{syn}:

$$\phi(t_0) = \phi_0 \quad \rightarrow \quad \phi(t_0 + T_{syn}) = \phi_0 \tag{1.4}$$

As the definitions rely on the **true anomalies** of celestial bodies, non-circular orbits mean that the same phasing does NOT imply the same relative positions between them. In other words, once the synodic period has passed, the phasing of the three considered bodies could result in a completely different relative positions with respect to the initial condition.
The problem needs to be reformulated. The goal is to find the period of time that elapses between a state of orbital positions of the bodies and the next occurrence of the same state. In literature, this particular period is called **period of orbital resonance** and it will be here indicated as T_{res}. Supposing that the orbits keep the other Keplerian elements unchanged during the revolution, the relation on true anomalies can be expressed as:

$$\begin{cases} \theta^{(1)}(t_0) = \theta_0^{(1)} \\ \theta^{(2)}(t_0) = \theta_0^{(2)} \\ \theta^{(3)}(t_0) = \theta_0^{(3)} \end{cases} \rightarrow \begin{cases} \theta^{(1)}(t_0 + T_{res}) = \theta_0^{(1)} \\ \theta^{(2)}(t_0 + T_{res}) = \theta_0^{(2)} \\ \theta^{(3)}(t_0 + T_{res}) = \theta_0^{(3)} \end{cases} \tag{1.5}$$

Since the true anomaly for an orbit repeats itself every orbital period T, it results:

$$\begin{cases} \theta_0^{(1)} = \theta^{(1)}(t_0 + iT^{(1)}) = \theta^{(1)}(t_0 + T_{res}) \\ \theta_0^{(2)} = \theta^{(2)}(t_0 + jT^{(2)}) = \theta^{(2)}(t_0 + T_{res}) \\ \theta_0^{(3)} = \theta^{(3)}(t_0 + kT^{(3)}) = \theta^{(3)}(t_0 + T_{res}) \end{cases} \rightarrow \quad T_{res} = iT^{(1)} = jT^{(2)} = kT^{(3)} \qquad (i,j,k \in \mathbb{N}) \tag{1.6}$$

As obtained in Equation 1.6, the resonance period T_{res} must be a multiple of all the three orbital periods. To find three compatible natural numbers for i, j, k, the following procedure can be followed:

$i = 1; \quad j = i \cdot T^{(1)}/T^{(2)}; \quad k = i \cdot T^{(1)}/T^{(3)}$
while $j \notin \mathbb{N}$ or $k \notin \mathbb{N}$ **do** ▷ a tolerance tol must be implemented
  $i = i + 1$
  $j = i \cdot T^{(1)}/T^{(2)}$
  $k = i \cdot T^{(1)}/T^{(3)}$
end while
return i, j, k

Note that, since a perfect resonance of three celestial bodies is realistically impossible, a certain tolerance tol must be introduced when evaluating $j, k \in \mathbb{N}$ in order to compute a reasonable T_{res}. In the specific case of this report, the execution of the above algorithm returned the following results:

tol	i (*Earth*)	j (*Mars*)	k (1036 *Ganymed*)
0.1159	13	6.9119	4.8841

Table 1.1: Results of the resonance analysis

T_{res} results to be 13 Earth's sidereal years, so the time domain can be restricted accordingly. It is important to keep in mind that this is an approximation, but since the mission has to departure in a reasonable date, it is acceptable to restrain the time window to the first 13 years. In any case, the cost of the mission will repeat similarly after 13 years.

1.4.2. Cost-plot analysis

The reduction of the departure time window in subsection 1.4.1 is a powerful but not sufficient restriction for the domain to analyze with Algorithm 1. Hence, a more detailed analysis has to be performed, including some restrictions for the first and second time of flight. The present paragraph presents and studies in detail two cost-plots. The first is related to the injection cost on the first Lambert's arc while the second exit cost is referred to the second Lambert's arc. Notice that the pork-chop plot of each leg can't be plotted, since the the two arcs are linked at the fly-by position. Given this consideration, the two cost plot obtained with the 13-year constrained departure window are following.

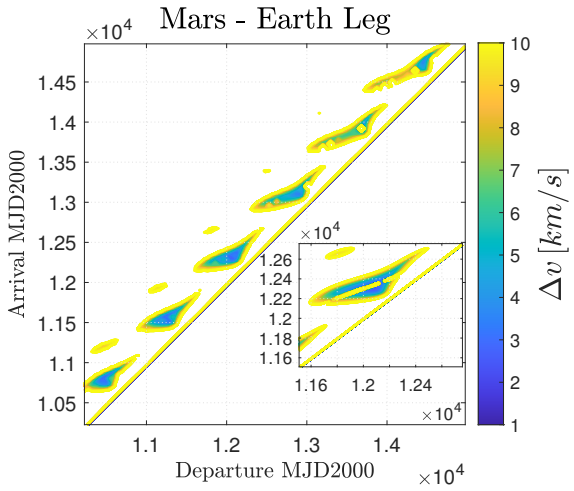

Figure 1.1: Cost plot for 1st leg

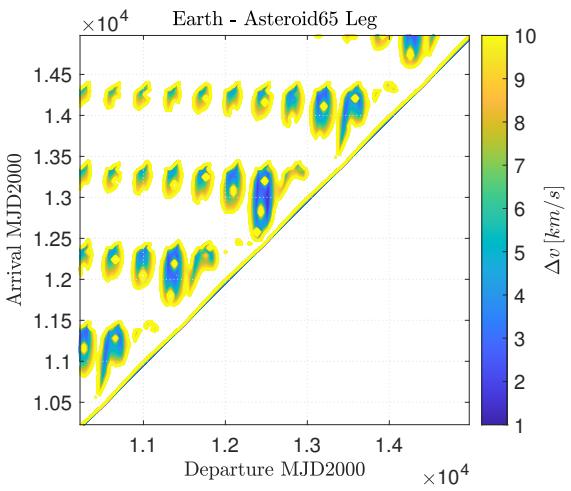

Figure 1.2: Cost plot for 2nd leg

The contour plot are set to a maximum value for the ΔV of 10 km/s, greater values are excluded since they wouldn't be relevant for the present study. Moreover, it was decided to use symmetrical time domains for departure and arrival, expressed in *mjd2000* units. Some important information can be retrieved from the contour plot of Figure 1.1:

- all the local minima that reach the lowest values are located along the diagonal, indicating that there is a constraint on the time of flight for the first arc. This behaviour is present also in the second arc Figure 1.2. Above the diagonal of both the plots the minima are higher Figure 1.2, or not existent Figure 1.1 for the set of contour lines considered. This is related to the fact that the Lambert's arc where calculated without considering the multi-revolution solutions subsection 1.2.2. Indeed, if the time of flight imposed is higher, the Lambert'arc solution will have a higher semi-major axis. This results in a higher ΔV to inject or exit the transfer arc since the energy difference between orbits becomes considerable. The solution that embraces multi-revolution arcs would benefit in this sense and could open new scenarios for the interplanetary arcs, as cited in [1].
- It can be noticed that a repetion pattern of the minima is present in both the figures. With particular emphasis on the Mars-Earth leg, the minimum shown as the blue-coloured zone, repeats every synodic period Table 1.2. This is due to the quasi-circular orbits of both the planets.
- A repetition pattern is noticeable also in Figure 1.2. To better analyze the plot, the values of the last three columns of Table 1.2 can be exploited. It can be noticed that the synodic period $T_{syn}^{E,G}$ can not explain the reoccurence of the minima while the resonance periods are both meaningful. The high tolerance resonance period $T_{res,1}^{E,G}$ fits all the repeated minima along the diagonal. The low tolerance resonance period $T_{res,2}^{E,G}$ can catch a lower frequency pattern, appreciable by focusing on the first and second-last *P-shaped* minima along the diagonal.
- Regarding the cost-plot of Earth-to-Mars transfer Figure 1.1, a particular behaviour of the minimum can be noticed on the zoomed box. The focus enables to appreciate a yellow ridge that separates the minimum zone in to two sub-area that contains mainly two minimum zones. As mentioned in [1], the two zones corresponds to two solutions for the Lambert's problem, in particular to the value of the transfer angle $\Delta\theta$. The upper zone corresponds to $\Delta\theta > \pi$ while the lower zone corresponds $\Delta\theta < \pi$. When $\Delta\theta = \pi$, since the orbital planes of Earth and Mars are not exactly coincident, the plane of the heliocentric transfer leg becomes almost perpendicular to the ecliptic, increasing the injection cost of the mission [2]. When the co-planar and circular assumption on Earth and Mars orbits is made, the central part of the minimum lobe in the zoomed box coincides with the Hohmann transfer [1].

$T_{syn}^{M,E}\ [mjd2000]$	$T_{syn}^{E,G}\ [mjd2000]$	$T_{res,1}^{E,G}$ (high tol) $[mjd2000]$	$T_{res,2}^{E,G}$ (low tol) $[mjd2000]$
779.9418	585.0697	1095.7711	2922.0562

Table 1.2: Results of the resonance analysis

From the observations presented above, it was decided to analyze the same cost plot but considering the time of flight on the y-axis, these values are bounded in a restricted domain. For the Earth-Mars transfer multiple and sub-multiple of the Hohmann transfer time. The hypothesis is reasonable since Mars and Earth have almost circular and co-planar orbits [3]. The same hypothesis can't be applied on the second heliocentric leg. This because Ganymed's orbit is inclined and highly eccentric, hence Hohmann's hypothesis doesn't hold.

1.4.3. Final time window selection

1.5. Conclusion and results

[4]

2. Planetary mission

Bibliography

[1] Davide Menzio. Grid-search applications for trajectory design in presence of flybys. PhD Dissertation, 2019. Site: https://www.politesi.polimi.it/handle/10589/152568.

[2] Richard Battin. *An introduction to the mathematics and methods of astrodynamics*. AIAA Education Series, 1987.

[3] Gianmarco Radice Pierluigi Di Lizia. Advanced global optimisation tools for mission analysis and design. Paper, 2004. Site: https://www.esa.int/gsp/ACT/resources/act_papers.

[4] Howard D. Curtis. *Orbital Mechanics for Engineering Students*. Elsevier, 2014.